CHAPTER 2

PROTON AND ELECTRON THRESHOLD ENERGY MEASUREMENTS FOR EXTRAVEHICULAR ACTIVITY SPACE SUITS

M. F. Moyers, G. D. Nelson
Dept. of Radiation Medicine
Loma Linda University
Loma Linda, California

P. B. Saganti
Space Radiation Health Project
NASA Johnson Space Center
Houston, Texas

PROTON AND ELECTRON THRESHOLD ENERGY MEASUREMENTS FOR EXTRAVEHICULAR ACTIVITY SPACE SUITS

ABSTRACT

Construction of ISS will require more than 1000 hours of EVA. Outside of ISS during EVA, astronauts and cosmonauts are likely to be exposed to a large fluence of electrons and protons. Development of radiation protection guidelines requires the determination of the minimum energy of electrons and protons that penetrate the suits at various locations. Measurements of the water-equivalent thickness of both U.S. and Russian EVA suits were obtained by performing CT scans. Specific regions of interest of the suits were further evaluated using a differential range shift technique. This technique involved measuring thickness ionization curves for 6-MeV electron and 155-MeV proton beams with ionization chambers using a constant source-to-detector distance. The thicknesses were obtained by stacking polystyrene slabs immediately upstream of the detector. The thicknesses of the 50% ionizations relative to the maximum ionizations were determined. The detectors were then placed within the suit and the stack thickness adjusted until the 50% ionization was reestablished. The difference in thickness between the 50% thicknesses was then used with standard range-energy tables to determine the threshold energy for penetration. This report provides a detailed description of the experimental arrangement and results.

2.1 INTRODUCTION

Construction of ISS will require more than 1000 hours of EVA. Outside of ISS during EVA, astronauts and cosmonauts are likely to be exposed to a significant fluence of electrons and protons. **Figures 2-1 and 2-2** contain typical energy spectra of electrons and protons anticipated at the orbit of ISS. When the current-generation EVA suits were designed, the architects had not envisioned the multitude of extensive-duration EVAs required for ISS construction, and radiation shielding was not of paramount importance. Radiation protection guidelines are therefore required before construction of ISS may commence in earnest. These guidelines will be based on calculational models that require validation. Achieving direct measurements of the minimum energy of electrons and protons that

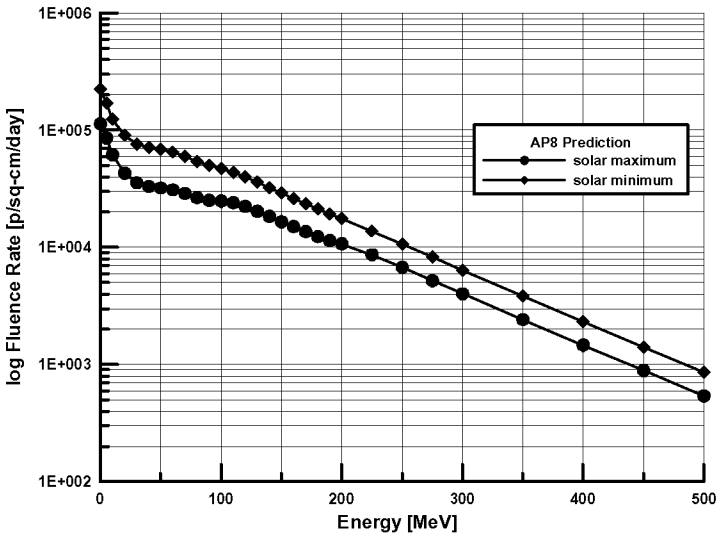

Figure 2-1. Typical electron spectra at the orbit of ISS predicted using the AE8 simulation. The circles represent the fluence rate at solar maximum while the diamonds represent the fluence rate at solar minimum. (Data courtesy of Ed Semones, NASA Johnson Space Center.)

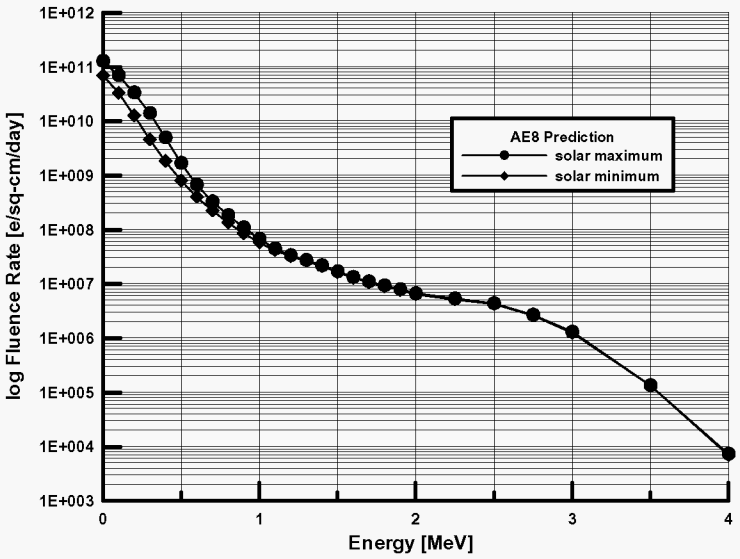

Figure 2-2. Typical proton spectra at ISS orbit predicted using the AP8 simulation. The circles represent the fluence rate at solar maximum while the diamonds represent the fluence rate at solar minimum. (Data courtesy of Ed Semones, NASA Johnson Space Center.)

can penetrate the suits at various locations is one of the validation steps. Additionally, these measurements may influence the designs of future space suits.

CT scans provided maps of the water equivalent thickness of both U.S. and Russian EVA suits. The minimum energy of electrons and protons that can penetrate these thicknesses were interpolated from standard range-energy tables. Specific regions of interest of the suits were evaluated directly with electron and proton beams, using a differential range shift technique.

2.2 METHODS AND MATERIALS

2.2.1 Suit Configurations

We studied both U.S. and Russian EVA suits. The U.S. suit is referred to as the EMU, the Russian suit as the Orlan-M. The EMU consists of many interchangeable parts that are combined to fit individual astronauts. **Tables 2-1** and **2-2** give the published composition and thicknesses of various components of the EMU helmet and extremities, respectively.

The helmet and EVVA, seen in **Figure 2-3**, consists of several layers, including an inner polycarbonate pressure bubble, a protective visor, a gold-plated sun visor, and an eyeshade. The majority of the suit covering the extremities, seen in **Figure 2-4**, consists of twelve layers, including a urethane-coated

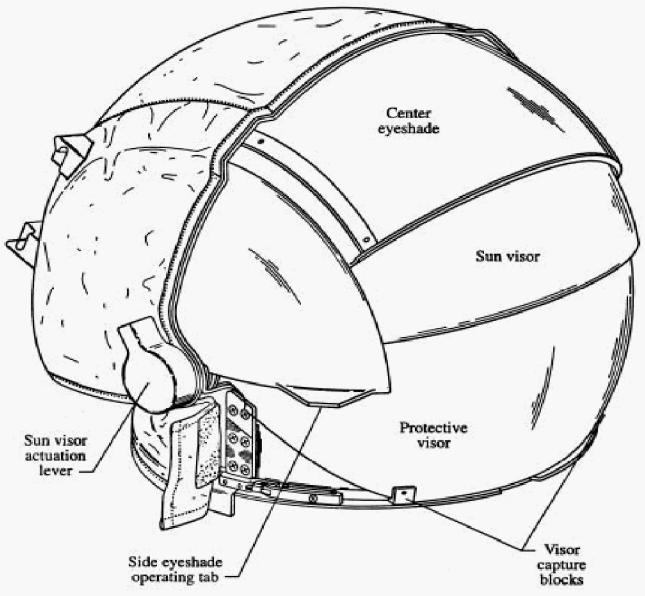

Figure 2-3. U.S. helmet and extravehicular visor assembly showing placement of visors and sunshades.

nylon to hold pressure, aluminum for thermal insulation, Kevlar for micrometeoroid protection, and water-filled tubing for cooling. The suit material covering the upper torso is the same as over the extremities except that a hard fiberglass shell having a thickness between 0.075" to 0.125" (0.10" avg.) is substituted for the pressure bladder and pressure-restraint layers.

The Orlan-M is a single-piece unit that comes in only one size but which, with cinch straps, can accommodate a limited range of different-size cosmonauts. The chest and abdomen of the Orlan contains a hard aluminum shell with entry provided via a door at the rear. The EMU provided for this experiment consisted of a mixture of training and flight-qualified parts. Sham backpacks were attached to each suit. Both suits were loaded with cooling liquid throughout the measurements, but were not pressurized.

Table 2-1. Configuration for Helmet/Extravehicular Visor Assembly of Extravehicular Mobility Unit
Data taken from Kosmo (1989). Materials listed from inside to outside.

Item	Material	Thickness [in]	Density Thickness [g/cm^2]
protective bubble	polycarbonate	0.06	0.182
ventilation pad	not available	not available	not available
protective visor	polycarbonate	0.06	0.182
sun visor	polysulfone with gold coating	0.06	0.190
sun shade	polycarbonate	0.06	0.182
back shell	polycarbonate	0.125	0.381
back thermal meteoroid garment	Teflon liner 5 plies non-woven Dacron 5 plies aluminized Mylar Teflon/Nomex/Kevlar	0.01 0.03 0.02 0.02	0.028 0.011 0.004 0.049

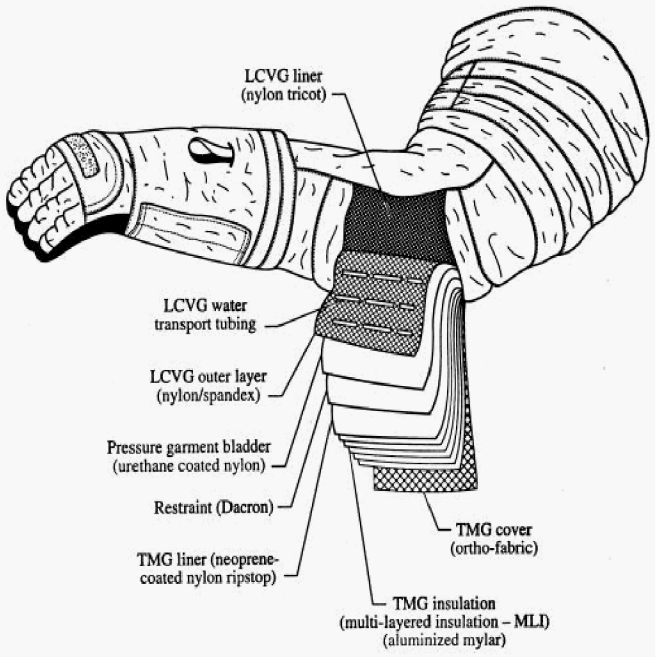

Cross section of material layup used for fabric for the arms and legs of the spacesuit.

Figure 2-4. U.S. EMU soft suit components showing multilayer fabrication.

Table 2-2. Configuration for Arms and Lower Torso of Extravehicular Mobility Unit (Data taken from Kosmo (1989)). *Materials listed from inside to outside.*

Item	Material	Thickness [in]	Density Thickness [g/cm^2]
undergarment	Capilare	not available	not available
liquid coolant vent garment	Nylon chiffon Nylon Spandex 1/16" ethylvinyl acetate tubing for H_2O	0.02	0.154
pressure bladder layer	Urethane-coated Nylon ripstop	0.011	0.014
pressure restraint layer	Dacron polyester	0.011	0.021
thermal meteoroid garment	Neoprene coated Nylon ripstop 5 plies aluminized Mylar Teflon/Nomex/Kevlar	0.009 0.025 0.02	0.028 0.014 0.049

2.2.2 Phantom

An anthropomorphic phantom was installed inside each suit during CT scanning and most threshold measurements in order to maintain the shape of the suit similar to its condition during an EVA. The Phantom Laboratory (Salem, New York) specially made the phantom for LLU with several cavities and inserts to accommodate various detectors and biological samples. As seen in **Figure 2-5**, the phantom spanned the top of the head to just above the knees and was cut transversely to provide 12 slices. The phantom also had two arms, removable at the shoulders, which were inflexible and stopped at the wrists. Most of the phantom consisted of a tissue-equivalent plastic with a composition by weight, as stated by the manufacturer, of 9.18% hydrogen, 67.78% carbon, 2.50% nitrogen, 20.31% oxygen, and 0.22% antimony.

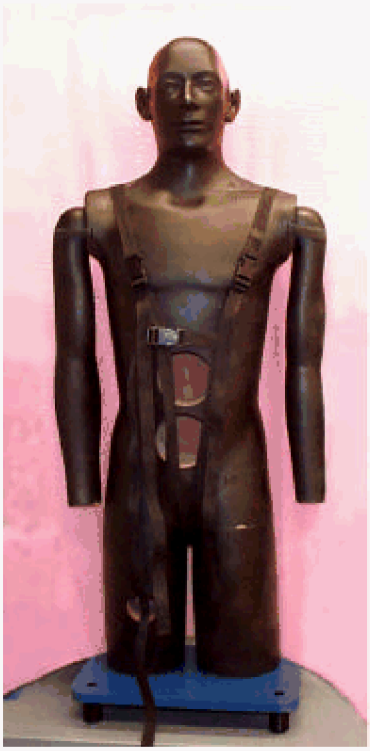

Figure 2-5. Anthropomorphic phantom used to simulate astronauts and cosmonauts inside EVA suits.

Figure 2-6. Anthropomorphic phantom in Orlan-M space suit as seen from back through entry door. Phantom is wearing the liquid-cooled ventilation garment.

LLU measurements of rectangular blocks of this material manufactured at the same time as the phantom yielded a density of 1.002 g/cm^3. Molded within the phantom were a human skeleton, various air cavities, and low-density polymeric foam to simulate lung tissue. The measured density of the lung material was 0.305 g/cm^3. **Figure 2-6** shows the phantom inside the Orlan suit with the liquid-cooled ventilation garment installed.

Figure 2-7. Feet first entry of EMU suit with sham backpack into the CT scanner. The arms are raised over the head to facilitate chest entry into the scanner aperture. Additional scans were performed to accommodate the helmet and gloves.

2.2.3 CT-Based Measurements

We performed CT scans with a General Electric 9800 scanner. **Figure 2-7** shows the EMU being scanned feet first. **Figure 2-8** shows the Orlan being scanned headfirst. The image reconstruction area was 480 mm in diameter with a transit bore of 690 mm. The reconstructed images consisted of 512 by 512 pixels per slice. Due to the presence of metal within the suits, we performed all scans using the highest available photon energy, 140 kVp. Other scanning parameters were: a tube current of 140 mA, slice thickness of 3 mm, and 10-mm distance between slice centers. We transferred the image data to a radiotherapy treatment planning system (TPS) to determine the water equivalent thickness at multiple locations.

Figure 2-8. Headfirst entry of Orlan-M suit with sham backpack into the CT scanner. A second scan was performed headfirst to accommodate the lower torso.

After entry into the TPS, image segmentation was performed by manual contouring. We simulated energy deposition distributions with 155-MeV proton beams from a variety of directions, using a TPS tool to interrogate the integral water equivalent path length across sample locations, and then using standard range-energy tables (ICRU, 1984; Janni, 1982) to determine the threshold energy for penetration.

2.2.4 Electron and Proton Measurements

The source of electrons for determining the threshold energy was a Siemens KD-2 electron accelerator (Siemens Medical Systems, Concord, California). The source of protons was the Loma Linda University Proton Treatment Facility (LLUPTF) (Moyers, 1999). We first measured the thickness ionization curves for nominal energy 6-MeV electron and 155-MeV proton beams without the suits with a 0.07-cm^3 thimble ionization chamber (Capintec, Nashville, Tennessee) using a constant source-to-detector distance and a stack of polystyrene slabs. The slope of the ionization versus thickness curve at the distal edge was then calculated. Next, we determined the thickness of the polystyrene stack, or range shifter, in terms of water equivalence (Moyers, 1992), needed to obtain an ionization nearly 50% of the maximum ionization. This thickness is called the "reference thickness" or T_R. We

then placed the detectors within the suit at the same distance from the source and adjusted the stack thickness until the 50% ionization was reestablished to within 1 mm of thickness. The water equivalent thickness is called the "sample thickness" or T_S. The thickness of the suit material was calculated using Equation 1.

$$\text{Suit Thickness} = (T_R - T_S) + \frac{(RI_R - RI_S)}{\text{Gradient}} \qquad \text{(Eq. 1)}$$

where: $RI_R \equiv$ relative ionization at reference thickness

$RI_S \equiv$ relative ionization at sample thickness

and Gradient ≡ slope on the distal edge of the ionization versus thickness curve.

The water equivalent thickness of the suit was thus the difference in relative ionizations divided by the gradient added to the difference in block thicknesses. This thickness was then used with standard range-energy tables (ICRU, 1984; Janni, 1982) to determine the threshold energy for penetration. Standard range-energy tables (ICRU, 1984; Janni, 1982) were used to determine the threshold energy for penetration from the measured suit thickness. In order for these measurements to be performed at any suit and gantry position, special extension cones were constructed to position the polystyrene slabs within the beam. These cones allowed for the stacking of polystyrene slabs within 20 mm of the suit surface.

Figure 2-9. Orlan-M suit in position with Siemens KD-2 linear electron accelerator for determining the threshold energy of electrons needed to penetrate the helmet. The beam is entering from the lower left through the cone containing the polystyrene rangeshifter plates.

Figure 2-10. EMU suit in position in LLUPTF gantry #1 for determining the threshold energy of protons needed to penetrate the neck region where the hard upper torso connects to the helmet assembly. The beam enters from the upper right through the cone containing the polystyrene rangeshifter plates. The cable entering the large hole at the bottom of the torso is attached to the ionization chamber. On the lower left is an electronic digital imaging device used for aligning patients during proton therapy.

Figure 2-9 shows the setup with the KD-2 electron accelerator for determining the threshold energy of electrons for penetrating the Orlan helmet. **Figure 2-10** shows the setup with gantry #1 of the LLUPTF for determining the threshold energy of protons penetrating the neck region of the EMU.

Alignment of the ionization chamber with the beam was usually performed visually using the treatment unit's internal light field or alignment lasers. Certain locations within the suit occasionally prevented the use of these methods. In these cases, radiographs were made to localize the chamber.

Figure 2-11 shows a radiograph of the thimble ionization chamber inside a finger of a glove.

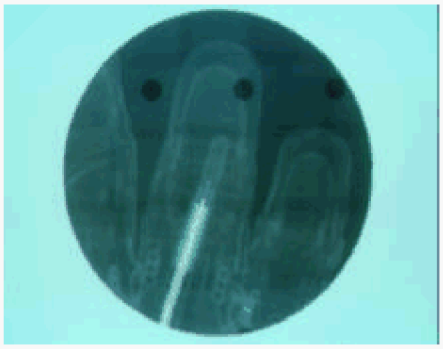

Figure 2-11. Radiographic image of the small thimble ionization chamber within a finger of a glove. The image shows that the detecting volume is at the middle phalanx of the ring finger.

2.3 RESULTS AND DISCUSSION

The CT planning resulted in 36 measurements. **Table 2-3** is a listing of the locations where useful water equivalent thickness measurements could be determined from the CT scans. The "swatch" refers to a flat sample of soft laminated suit material used to cover the extremities and abdomen. Glove thickness measurements were made from the dorsal direction only, as the astronaut will normally be carrying a tool or gripping a handhold that offers protection to the ventral side.

Figure 2-12 is a slice through the abdomen of the phantom where the HUT connects to the lower half of the suit using a metal ring. **Figure 2-13** is an example plan showing a 155-MeV, 60-mm modulated proton beam entering the helmet from the superior/anterior direction. **Figure 2-14** shows a plan of a 155 MeV proton beam entering the U.S. suit from the posterior direction. The suit piece being measured in this case was the HUT that is formed out of fiberglass. **Table 2-3** also gives the results of the CT water equivalent measurements and the calculated electron and proton threshold energies.

Figure 2-12. XCT image of the abdominal region of the phantom within the EMU. The cone-shaped lines from the middle to anterior aspect of the phantom are formed by a removable cylinder inserted into a hole in the phantom. The bright dots around the circumference are ball bearings at the joint of the hard upper torso and the lower suit allowing rotation of the suit just above the hips. The bright object above the phantom is the metal connecting buckle for the liquid carrying tubes flowing from the back pack to the liquid-cooling ventilation garment.

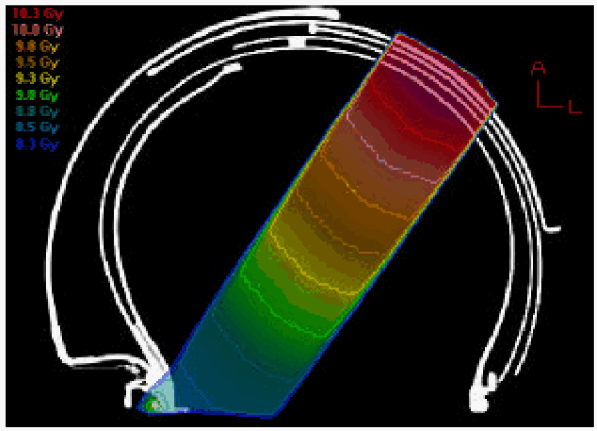

Figure 2-13. A sagittal XCT scan and plan of the U.S. helmet and extravehicular visor assembly. The astronaut's face would be to the right of the image and the back of the head to the left. A simulated 155-MeV proton beam enters from the anterior/superior direction passing through the eye shade, sun visor, protective visor, and bubble. At 155 MeV, very little protection is afforded by the thin plastic layers.

Table 2-3. Electron and Proton Threshold Energies Derived From CT Water-Equivalent Measurements

Sample Location Code	Location Description	Thickness [mm H2O]	Electron Energy [MeV]	Proton Energy [MeV]
C1.	EMU swatch	1.8 min.	0.51	12.3
C2.	Orlan swatch	2.4 min.	0.62	14.4
C3.	EMU helmet, anterior / superior entrance			
a.	sun shade	3.0	0.74	16.3
b.	sun visor	2.0	0.55	13.0
c.	protective visor	1.3	0.40	10.2
d.	bubble	1.7	0.48	11.9
C4.	EMU helmet, posterior entrance			
a.	back shell	3.6	0.86	18.1
b.	bubble	1.9	0.53	12.6
c.	ventilation pad	4.5	1.02	20.5
C5.	EMU glove, dorsal entrance	2.2	0.59	13.7
C6.	Orlan glove, dorsal entrance	1.1	0.36	9.3
C7.	EMU HUT, left posterior entrance	3.3	0.80	17.2
C8.	EMU HUT, right posterior entrance	4.4	1.01	20.2
C9.	Orlan helmet, right lateral entrance			
a.	outer	2.8	0.70	15.7
b.	middle	2.7	0.68	15.4
c.	inner	4.0	0.93	19.1
C10.	Orlan helmet, left lateral entrance			
a.	outer	2.4	0.63	14.4
b.	middle	2.8	0.70	15.7
c.	inner	4.3	0.99	20.0
C11.	EMU helmet, posterior entrance			
a.	back shell	5.0	1.12	21.7
b.	sun shade	2.5	0.65	14.7
c.	sun visor	2.4	0.63	14.4
d.	bubble	3.5	0.84	17.8
e.	ventilation pad	4.0	0.93	19.1
C12.	EMU helmet, right lateral entrance, bubble	2.0	0.55	13.0
C13.	EMU helmet, posterior entrance			
a.	back shell	3.6	0.86	18.1
b.	bubble	3.6	0.86	18.1
c.	ventilation pad	4.3	0.99	20.0
C14.	EMU, posterior hip entrance	2.1	0.57	13.3

Two issues need to be discussed with respect to the CT planning. The first concerns the large amount of steel in the suits and associated equipment. For the photon energies used by the CT scanner, steel completely absorbs some photons via the photoelectric effect and scatters other photons at large angles via Compton scattering. Both processes result in the production of artifacts during image reconstruction, increasing the uncertainty of the thickness measurements. The second issue is the presence of the sham backpacks. The initial experiment design did not include these. As seen in **Figures 2-12 and 2-14**, their presence forced some suit components to extend beyond the reconstruction circle. Some components also intruded into the space reserved for calibrating the CT detectors, resulting in additional artifacts and uncertainties.

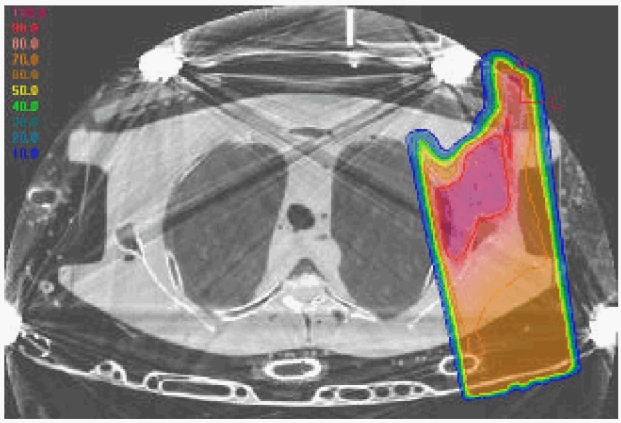

Figure 2-14. An axial XCT scan and plan of the U.S. hard upper torso through the phantom's chest. The lungs, ribcage, and spinal vertebrae may be seen. The arms were not attached to the phantom for this scan. Artifacts from the metal components of the suit are easily seen. A simulated 155-MeV proton beam enters the phantom's back shoulder passing through the hard upper torso.

Figures 2-15 and 2-16 show, respectively, the electron and proton range ionization curves for the electron and proton beams using the range shifter blocks and a constant source-to-detector distance. The solid lines are linear fits along the distal edges. The ionization gradient at the distal edge is 6.3% per mm for the electron beam and 23.4% per mm for the proton beam.

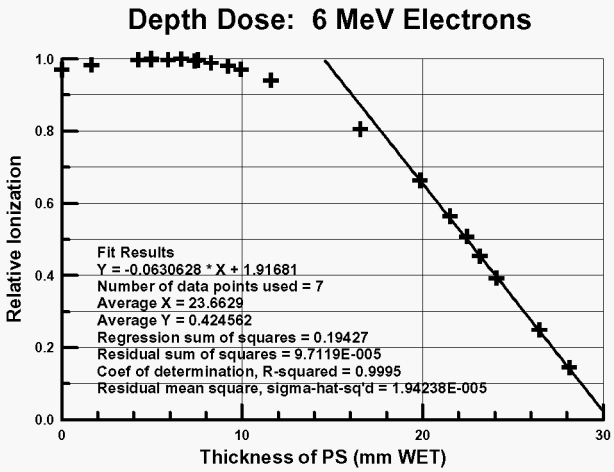

Figure 2-15. Ionization versus range shifter thickness for the 6 MeV electron beam. The thickness is given in terms of water equivalent thickness. Plotted crosses represent the measured ionization. The solid line is a fit through the 7 points on the distal edge. Results of the linear fitting are also given.

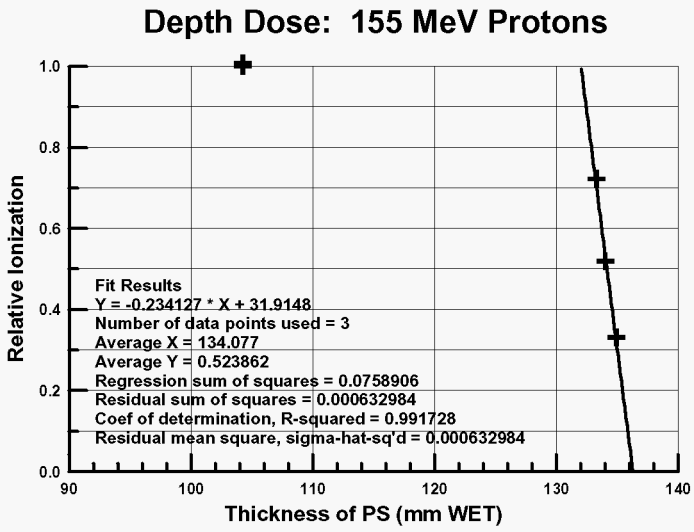

Figure 2-16. Ionization versus range shifter thickness for the 155-MeV proton beam. The thickness is given in terms of water equivalent thickness. Plotted crosses represent the measured ionization. The solid line is a fit through the 3 points on the distal edge. Results of the linear fitting are also given.

There were 33 thickness measurements at 20 locations with the electron beam (**Table 2-4**). The derived energies are given in **Table 2-5**. Sample locations listed as "a" and "b" represent different reference or sample depths for the measurement but the same suit location.

Table 2-4. Coding for Electron Measurement Locations

Code	Description
E1.	U.S. glove, right hand, ring finger, middle phalanx, dorsal entrance
E2.	U.S. glove, right hand, ring finger, proximal phalanx, dorsal entrance
E3.	U.S. glove, right hand, index finger, middle phalanx, dorsal entrance
E4.	Russian glove, right hand, ring finger, middle phalanx, dorsal entrance
E5.	Russian glove, right hand, ring finger, proximal phalanx, dorsal entrance
E6.	Russian glove, right hand, index finger, middle phalanx, dorsal entrance
E7.	U.S. helmet, bubble+protective visor, anterior entrance
E8.	U.S. helmet, bubble+ventilation pad+retracted sun visor+retracted sun shade, posterior entrance
E9.	U.S. helmet, bubble+ventilation pad (sun visor and sun shade forward), posterior entrance
E10.	U.S. helmet/upper torso ring, left anterior entrance
E11.	U.S. upper left arm
E12.	U.S. HUT, right lateral entrance
E13.	U.S. swatch
E14.	Russian swatch
E15.	Russian helmet, bubble, anterior entrance
E16.	Russian helmet, bubble+ sun visor, anterior entrance
E17.	Russian hard torso (chest), anterior entrance
E18.	Russian left elbow patch, dorsal entrance
E19.	U.S. boot, middle phalanx, inferior entrance
E20.	U.S. boot, middle phalanx, superior entrance

Although the U.S. and Russian gloves appear very thin, they are at the limit of this measurement technique for electrons. The thin finger covering was deemed necessary during the glove design for dexterity so that the astronauts could grab handholds placed on the outside of the station and manipulate various tools and station components. When incident upon flat surfaces, the resolving power of the electron beam is about 0.4 mm or 0.08 MeV.

When measuring surfaces having curves and folds, thickness averaging occurs as a result of range straggling and the uncertainty increases. Another source of uncertainty is due to an unknown source-to-detector distance when the detector is installed within the suit. This effect should be less than 4% however, which would translate to a maximum error in thickness of 0.7 mm or 0.14 MeV.

There were 33 thickness measurements at 19 locations with the proton beam (**Table2-6**). The derived energies are given in **Table 2-7**. The glove measurements appear thicker in the proton beam than the electron and provide a closer match to the CT results. The resolving power of the proton beam is about 0.1 mm when incident upon flat surfaces. Because the protons are heavier than electrons, they do not scatter as much, resulting in less thickness averaging due to range straggling. One source of error, although small, is that the water equivalence of the blocks was measured at energies higher than found near the distal edge where the suit was placed. This should result in at most a 2% error in the thickness.

Table 2-5. Electron Threshold Measurements

The sample thickness is reported in terms of water equivalent thickness.

Sample Location	Ref Depth [mm]	Sample Depth [mm]	R-S Depth [mm]	Ref Depth Dose	Sample Depth Dose	R-S Depth Dose	Grad Reduc [mm]	Sample Thickness [mm]	Electron Energy [MeV]
E1a	22.99	22.99	+0.00	0.5076	0.4705	+0.0371	+0.59	0.59	0.23
E1b	22.99	22.09	+0.90	0.5076	0.5490	-0.0414	-0.66	0.24	0.13
E2	22.99	22.09	+0.90	0.5076	0.4989	+0.0087	+0.14	1.04	0.34
E3a	22.99	22.09	+0.90	0.5076	0.4939	+0.0137	+0.22	1.12	0.36
E3b	22.99	21.18	+1.81	0.5076	0.5702	-0.0626	-0.99	0.82	0.29
E4a	22.99	23.85	-0.86	0.5308	0.4767	+0.0541	+0.86	0.00	N/A
E4b	22.99	22.09	+0.90	0.5308	0.6433	-0.1125	-1.79	-0.89	N/A
E5a	22.99	23.85	-0.86	0.5308	0.4325	+0.0983	+1.56	0.70	0.26
E5b	22.99	22.99	+0.00	0.5308	0.5079	+0.0229	+0.36	0.36	0.17
E6a	22.99	23.85	-0.86	0.5308	0.4694	0.0614	+0.97	0.11	0.09
E6b	22.99	22.99	+0.00	0.5308	0.5461	-0.0153	-0.24	-0.24	N/A
E7a	21.18	18.82	+2.36	0.4930	0.4548	+0.0382	+0.61	2.97	0.73
E7b	21.18	17.91	+3.27	0.4930	0.5057	-0.0127	-0.20	3.07	0.76
E8	21.18	8.65	+12.53	0.4930	0.4882	+0.0048	+0.08	12.61	2.53
E9	21.18	12.22	+8.96	0.4930	0.5216	-0.0286	-0.45	8.51	1.76
E10	21.18	0.0	+21.18	0.4930	0.2050	+0.2880	+4.73	25.75	5.05
E11a	21.18	15.25	+5.93	0.4930	0.4489	+0.0441	+0.70	6.63	1.42
E11b	21.18	14.34	+6.84	0.4930	0.5347	-0.0417	-0.66	6.18	1.33
E12a	21.18	18.82	+2.36	0.4930	0.4816	+0.0114	+0.18	2.54	0.65
E12b	21.18	17.91	+3.27	0.4930	0.5432	-0.0502	-0.80	2.47	0.64
E13a	22.99	22.99	+0.00	0.5083	0.4453	+0.0630	+1.00	1.00	0.34
E13b	22.99	22.09	+0.90	0.5083	0.5105	-0.0022	-0.03	0.87	0.31
E14a	22.99	22.99	+0.00	0.5083	0.4009	+0.1074	+1.70	1.70	0.49
E14b	22.99	21.18	+1.81	0.5083	0.5358	-0.0275	-0.44	1.37	0.42
E15	22.99	19.72	+3.27	0.5083	0.5092	-0.0009	-0.01	3.26	0.79
E16	22.99	16.15	+6.84	0.5083	0.5017	+0.0066	+0.11	6.95	1.48
E17	22.99	4.47	+18.52	0.5083	0.5017	+0.0066	+0.10	18.62	3.67
E18a	22.99	15.25	+7.74	0.5083	0.4952	+0.0131	+0.21	7.95	1.66
E18b	22.99	14.34	+8.65	0.5083	0.5294	-0.0211	-0.33	8.32	1.73
E19a	22.99	5.38	+17.61	0.5083	0.4915	+0.0168	+0.27	17.88	3.52
E19b	22.99	4.47	+18.52	0.5083	0.5580	-0.0497	-0.79	17.73	3.49
E20a	22.99	20.28	+2.71	0.5083	0.4937	+0.0146	+0.23	2.94	0.73
E20b	22.99	19.72	+3.27	0.5083	0.5296	-0.0213	-0.33	2.94	0.73

Energy: 6 MeV Electron Depth Dose Gradient at 50% = 0.063/mm

Table 2-6. Coding for Proton Measurement Locations

Code	Description
P1.	U.S. swatch
P2.	Russian swatch
P3.	U.S. helmet, bubble+protective visor (sun visor and sun shade retracted), anterior entrance
P4.	U.S. helmet, bubble+protective visor+sun visor (sun shade retracted), anterior entrance
P5.	U.S. helmet, bubble+ventilation pad+retracted sun visor+retracted sun shade, posterior entrance
P6.	U.S. glove, right hand, ring finger, middle phalanx, dorsal entrance
P7.	U.S. glove, right hand, ring finger, proximal phalanx, dorsal entrance
P8.	U.S. glove, right hand, index finger, middle phalanx, dorsal entrance
P9.	Russian glove, right hand, ring finger, distal phalanx, dorsal entrance
P10.	Russian glove, right hand, ring finger, middle phalanx, dorsal entrance
P11.	U.S. boot, middle phalanx, superior entrance
P12.	U.S. boot, middle phalanx, inferior entrance
P13.	U.S. helmet/upper torso ring, left anterior entrance
P14.	U.S. HUT, right lateral entrance
P15.	U.S. arm
P16.	Russian helmet, bubble, anterior entrance
P17.	Russian helmet, bubble+ sun visor, anterior entrance
P18.	Russian left elbow patch, dorsal entrance
P19.	Russian hard torso (chest), anterior entrance

Another possible advantage of the proton measurement technique compared to that using the electron beam is that the proton snout containing the range shifter blocks could be retracted away from the suit to better guarantee a constant source-to-detector distance. This may reduce the uncertainty due to detector positioning. The last column of **Table 2-7** is the threshold energy for electrons calculated using the sample thicknesses that were determined using the proton beams.

2.4 SUMMARY

The thickness of U.S. and Russian EVA suits were determined at various locations using a CT scanner, electron beam, and proton beam. From those measurements, the threshold energies for penetration by electron and proton beams were calculated. The results were provided to NASA so that they may perform validation of transport code calculations and risk estimations. The better resolving power, reduced scatter, and variable distance snout led to the conclusion that the proton thickness measurements should be used to calculate the electron threshold energies as well as the proton threshold energies. If the CT measurements were to be repeated to obtain a full map of the suit, a high-energy, large-bore scanner should be used to reduce the artifacts and cover all components. Lastly, one should consider adding a thin layer of material to the dorsal side of the gloves; this might result in a substantial reduction of dose to the fingers from low-energy electrons.

Table 2-7. Proton Threshold Measurements

The sample thickness is reported in terms of water equivalent thickness.

Sample Location	Ref Depth [mm]	Sample Depth [mm]	R-S Depth [mm]	Ref Depth Dose	Sample Depth Dose	R-S Depth Dose	Grad Reduc [mm]	Sample Thickness [mm]	Proton Energy [MeV]	Electron Energy [MeV]
P1	134.94	133.28	+1.66	0.5115	0.5155	-0.0040	-0.02	1.64	16.7	0.47
P2	134.94	132.35	+2.59	0.5115	0.5460	-0.0345	-0.15	2.44	17.7	0.63
P3a	134.35	130.61	+3.74	0.5190	0.4454	+0.0736	+0.31	4.05	19.3	0.94
P3b	134.35	129.71	+4.64	0.5190	0.6646	-0.1456	-0.62	4.02	19.2	0.93
P4a	134.35	128.85	+5.50	0.5190	0.4342	+0.0848	+0.36	5.86	23.7	1.28
P4b	134.35	127.95	+6.40	0.5190	0.6311	-0.1121	-0.48	5.92	23.8	1.29
P5a	134.35	121.11	+13.24	0.5190	0.4125	+0.1065	+0.46	13.70	37.9	2.73
P5b	134.35	120.20	+14.15	0.5190	0.6075	-0.0885	-0.38	13.77	38.0	2.74
P6	134.35	132.54	+1.81	0.5190	0.5015	+0.0175	+0.07	1.88	12.6	0.52
P7a	134.35	132.42	+1.93	0.5190	0.4361	+0.0829	+0.35	2.28	14.0	0.60
P7b	134.35	131.52	+2.83	0.5190	0.6033	-0.0843	-0.35	2.48	14.7	0.64
P8	134.35	132.54	+1.81	0.5190	0.5516	-0.0326	-0.14	1.67	11.7	0.48
P9a	134.35	132.42	+1.93	0.5190	0.4565	+0.0625	+0.27	2.20	13.7	0.59
P9b	134.35	131.52	+2.83	0.5190	0.6604	-0.1414	-0.60	2.23	13.8	0.59
P10a	134.35	132.54	+1.81	0.5190	0.5181	+0.009	+0.00	1.81	12.3	0.51
P10b	134.35	132.43	+1.93	0.5190	0.5842	-0.0652	-0.28	1.65	11.7	0.48
P11a	134.35	130.61	+3.74	0.5190	0.4659	+0.0531	+0.23	3.97	19.1	0.93
P11b	134.35	129.71	+4.64	0.5190	0.6446	-0.1256	-0.54	4.10	19.4	0.95
P12a	134.35	118.08	+16.27	0.5190	0.3823	+0.1367	+0.58	16.85	42.5	3.33
P12b	134.35	117.17	+17.18	0.5190	0.5781	-0.0591	-0.25	16.93	42.6	3.34
P13a	134.35	90.92	+43.43	0.5261	0.4271	+0.0990	+0.42	43.85	72.4	8.75
P13b	134.35	90.02	+44.33	0.5261	0.4772	+0.0489	+0.21	44.54	73.1	8.90
P14a	134.35	130.61	+3.74	0.5261	0.4860	+0.0401	+0.17	3.91	18.9	0.91
P14b	134.35	129.71	+4.64	0.5261	0.6826	-0.1565	-0.67	3.97	19.1	0.93
P15a	134.35	133.44	+0.91	0.4377	0.3340	0.1037	+0.44	1.35	10.4	0.41
P15b	134.35	132.54	+1.81	0.4377	0.5087	-0.0710	-0.30	1.51	11.1	0.45
P16a	134.35	129.71	+4.64	0.4377	0.3382	+0.0995	+0.43	5.07	21.9	1.13
P16b	134.35	128.85	+5.50	0.4377	0.5230	-0.0853	-0.36	5.14	22.0	1.14
P17a	134.35	127.95	+6.40	0.4377	0.3399	+0.0978	+0.42	6.82	25.8	1.45
P17b	134.35	127.04	+7.31	0.4377	0.5318	-0.0941	-0.40	6.91	26.0	1.47
P18a	134.35	128.85	+5.50	0.4377	0.4982	-0.0605	-0.26	5.24	22.3	1.16
P18b	134.35	127.95	+6.40	0.4377	0.6250	-0.1873	-0.80	5.60	23.1	1.23
P19	134.35	125.58	+8.77	0.4377	0.4407	-0.0030	-0.01	8.76	29.6	1.81

Energy: 155 MeV Proton Depth Dose Gradient = 0.234/mm

2.5 ACKNOWLEDGMENTS

This work was partially funded by NASA Cooperative Agreement #NCC9-79. These experiments were made possible by the contribution of many people. Steven Rightnar of LLU assisted with the performance and coordination of the experiments at LLU. Jack Miller of the Lawrence Berkeley Laboratories organized the experiments. Francis Cucinotta of the Johnson Space Center (JSC) sponsored the experiments. Robert Jones of Inland Technical Services, Inc. was responsible for fabricating the extension cone range shifter slab holders. The Phantom Laboratory constructed the special phantom and inserts to the specifications required for the experiments. Jason Poffenberger and Bill Welch of ILC Dover manipulated the phantoms and suits and assisted with the installation of the various detectors. Brett Geisel of Loma Linda University Medical Center (LLUMC) performed the CT scans. Ed Semones of JSC provided the electron and proton spectral data. The accelerator operators at LLU provided beam tuning during the various experiments. Mark Shavers of JSC assisted with editing the manuscript.

REFERENCES

International Commission on Radiation Units and Measurements (1984) "Radiation dosimetry: electron beams with energies between 1 and 50 MeV", ICRU Report **35** (International Commission on Radiation Units and Measurements, Bethesda, MD).

Janni J. F. (1982) Proton range-energy tables, 1 keV - 10 GeV. *Atomic Data and Nuclear Data Tables* **27(2/3):** 147-339.

Kosmo J. J., Nachtwey D. S., Hardy A. (1989) Candidate space station EVA space suit - radiation analysis final report. CTSD-SS-241.

Moyers, M. F. "Proton Therapy" The Modern Technology of Radiation Oncology: A Compendium for Medical Physicists and Radiation Oncologists ed. vanDyk, J. (Wisconsin: Medical Physics Publishing, 1999) p. 823-869.

Moyers M. F., Miller D. W., Siebers J. V., Galindo R., Sun S., Sardesai M., Chan L. (1992) Water equivalence of various materials for 155 to 250 MeV protons. Medical Physics 19(3) (1992) p. 829. Abstract.